Table 2. Peptide amidase catalyzed amidation of peptides in acetonitrile containing 5% of water.[a]

Peptide	Yield [%] of amide	Precipitation of ammonium salt	t_{ret} [min] amide	peptide
Z-Gly-Phe-OH	33.5	no	6.73	8.84
Z-Gly-Leu-OH	27.5	yes[b]	5.83	7.89
Z-Gly-Tyr-OH	1.0	yes	3.96	4.71
Z-Ala-Phe-OH	8.0	yes[c]	8.08	11.04
Z-Leu-Phe-OH	23.0	no	19.84	26.83
Z-Pro-Phe-OH	21.5	no	11.58	14.57
Z-Phe-Ala-OH	33.0	yes[b]	8.10	9.90
Z-Ala-Pro-Leu-OH	24.0	no	8.75	10.75

[a] 0.025 mmol of peptide, 0.035 mmol of NH_4HCO_3, 2 mg of amidase, 0.50 mL total volume, 72 h, 40 °C. [b] Precipitation after 40 h. [c] Immediate precipitation.

groups in peptides is possible. The necessary enzyme can be isolated from orange peel, a waste product of the juice industry, by a simple two-stage extraction procedure that yields 300 – 500 U per kilogram of peel.[9] Since the unchanged peptide can be easily recycled, enzymatic amidation could be economically feasable after further optimization.

Experimental Section

Typical procedure for the amidase-catalyzed amidation of peptides: The reactions were carried out in 2-mL plastic tubes with screw caps, which were incubated in a rotatory shaker at 1000 rpm and various temperatures. The benzyloxycarbonyl dipeptide (0.025 mmol) was dissolved in acetonitrile (475 μL). The required water and ammonium concentrations were adjusted by the addition of water and 2 M NH_4HCO_3 to give the final calculated volume of 500 μL. After the addition of lyophylized amidase (2 mg), the suspension was shaken at 40 °C for several days. Before the termination of the reaction, the apparent pH value of the mixture was checked with indicator paper. The reactions were terminated by diluting the mixture with 50% aqueous methanol (1.5 mL) containing 1% trifluoroacetic acid (TFA). The product yield was estimated by HPLC on an RP-18 column (Merck, WP-300, 5 μm, 25 × 0.4 cm) operated isocratically with a mixture of methanol and 0.1% TFA (45/55) at 1 mL min^{-1}. Detection was carried out at 254 nm. The newly formed peak corresponded to the peptide amide and had a retention time identical to that of a standard sample. To follow the course of the amidase-catalyzed amidation of Z-Gly-Phe-OH with time, reactions were performed in several test tubes and terminated after a given time interval.

Synthesis of Z-Gly-Phe-NH_2: Z-Gly-Phe-OH (357 mg, 1 mmol) was dissolved in a mixture of acetonitrile (19 mL) and water (0.3 mL). After a solution of NH_4HCO_3 (0.7 mL, 2 M) and amidase (80 mg) was added, the mixture was shaken in a sealed vessel at 35 °C for 4 d. According to HPLC analysis the yield of Z-Gly-Phe-NH_2 was 31%. The neutral product was isolated by cation- and anion-exchange chromatography and crystallized from ethyl acetate/petroleum ether to give 82 mg of dipeptide amide (23% yield, pure according to TLC and HPLC analysis). The m.p. of 133 – 134 °C corresponds to that of standard sample. Amino acid analysis: Gly 1.00, Phe 0.99; FAB-MS: 356.1 $[M+H]^+$.

The peptide amidase was isolated according to the literature procedure.[7, 9] The lyophilized enzyme had an activity of 0.2 U mg^{-1} with Z-Gly-Tyr-NH_2 as substrate. The peptides were purchased from Bachem (Germany), and ammonium salts were obtained from Fluka (Switzerland).

Received: February 10, 1998 [Z11456IE]
German version: *Angew. Chem.* **1998**, *110*, 1986 – 1989

Keywords: amides · enzymes · enzyme catalysis · peptides

[1] D. J. Merkler, *Enzyme Microb. Technol.* **1994**, *16*, 450 – 456.
[2] K. Breddam, F. Widmer, J. T. Johansen, *Carlsberg Res. Commun.* **1981**, *46*, 121 – 128.
[3] F. Widmer, K. Breddam, J. T. Johansen, *Carlsberg Res. Commun.* **1981**, *46*, 97 – 106.
[4] S.-T. Chen, M.-K. Jang, K.-T. Wang, *Synthesis* **1993**, 858 – 860.
[5] H.-D. Jakubke, P. Kuhl, A. Könnecke, *Angew. Chem.* **1985**, *97*, 79 – 87; *Angew. Chem. Int. Ed. Engl.* **1985**, *24*, 85 – 93.
[6] D. Steinke, M.-R. Kula, *Angew. Chem.* **1990**, *102*, 1204 – 1205; *Angew. Chem. Int. Ed. Engl.* **1990**, *29*, 1139 – 1140.
[7] D. Kammermeier-Steinke, A. Schwarz, C. Wandrey, M.-R. Kula, *Enzyme Microb. Technol.* **1993**, *15*, 764 – 769.
[8] V. Čeřovský, K. Martinek, *Collect. Czech. Chem. Commun.* **1989**, *54*, 2027 – 2041.
[9] U. Stelkes-Ritter, Dissertation, Universität Düsseldorf, **1994**.

Secondary Bonding between Chalcogens or Pnicogens and Halogens**

Gregory A. Landrum and Roald Hoffmann*

The more crystal structures we know, the clearer it becomes that in the solid state there are many contacts in the range between a bond and a van der Waals interaction. N. W. Alcock introduced the useful term "secondary bonding" for these, and formulated a set of rules for their occurrence and directionality.[1]

For electron-rich main-group systems there are two popular ways to address in a qualitative way the electronic structure of secondary bonded species—either as a manifestation of hypervalence (electron-rich three-center or multicenter bonding[2]) or as directional donor – acceptor bonding.[3] We feel these approaches are in fact equivalent, though we doubt that the number of energetic electrons expended on the demerits of one or the other chemical views is exhausted.

In recent work we have used the concept of donor – acceptor interactions to interpret calculations on hypervalent bonding in the trihalides and hydrogen bihalides,[4] intermolecular interactions in R_2QX_2 (Q = Se, Te; X = I, Br, Cl),[5] and the secondary bonding in dimers of Ph_2IX and XF_3 (X = I, Br, Cl).[6] These studies, and the importance of directionality in secondary bonding,[7] have led us to look more broadly at the nature of secondary interactions. In this work searches of the Cambridge Structural Database[8] (CSD) have been used to determine the prevalence and geometries of secondary bonding in crystals containing chalcogens or Group 15

[*] Prof. Dr. R. Hoffmann, Dr. G. A. Landrum[+]
Chemistry and Materials Science Center
Cornell University, Ithaca, NY, 14853 – 1301 (USA)
Fax: (+1) 607-255-5707

[+] Current address
Institut für Anorganische Chemie, Technischen Hochschule
Professor-Pirlet-Strasse 1, D-52074 Aachen (Germany)

[**] We are grateful to the National Science Foundation for its support of our work through Research Grant CHE 94 – 08455. We would also like to thank Silicon Graphics for their generous donation of the computer hardware which was used in this work. In the process of preparing this work, we benefited greatly from insightful comments by Hans-Beat Bürgi.

  1433-7851/98/3713-1887 $ 17.50+.50/0

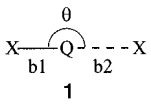

1

elements (pnicogens) as one interacting group and halides as the other.[9] The arrangement of atoms used in our search of the CSD is sketched in **1**. The restrictions we imposed are that $b1$ be indexed as a bond (of any type) in the database, $b2$ is any kind of contact (bonded or "nonbonded", inter- or intramolecular) less than 4.5 Å in length, and θ has a value between 150 and 180° (one of Alcock's rules points to the approximate colinearity of primary and secondary bonds; actually the multitudinous polyiodide structures known to us show that colinearity is not essential—it is the overlap of donor and acceptor functions that is determinative). To maintain as much generality as possible, no restrictions were placed upon either the oxidation state or coordination numbers of the atoms involved in the bonds.

All CSD searches were carried out using the Quest software provided with the database. The total data set obtained was of nontrivial size (almost 3000 entries). The data were post-processed with "custom" software to ensure that $b1$ is less than or equal to $b2$ (by switching the two values if necessary), to calculate bond asymmetry parameters, and to remove duplicate entries.

While CSD searches were carried out for all possible combinations of Q = As, Sb, Bi, Se, Te; X = F, Cl, Br, I, for reasons of brevity, and because the data sets show similar features, only two sets of results will be discussed here: the full X series for Q = Sb and Te.

Figure 1 shows the scatter plots of $b1$ and $b2$ for the Q = Sb, Te; X = F, Cl, Br, I systems. Some features are immediately apparent: First, for Q = Sb, the bond pairs observed appear to be grouped into two distinct sets. The first, lying close to the line $b1 = b2$, connects to the second set at large values of $b1$. The graph for Set 2 curves upward sharply as $b1$ gets shorter. In order to show the data as compactly as possible the scales for the $b1$ and $b2$ distances are different. The presence of two sets of bond-pair types in the scatter plots of Figure 1, in contrast to the single set (corresponding to Set 2) observed in earlier structural database studies,[9a,9e] is due to the generality of the search criteria used. The restrictions on oxidation state and coordination number or both used in earlier work rule out the appearance of Set 1, which is composed almost exclusively of Sb^{5+} compounds.

The plots for Q = Sb with X ≠ F all show similar curved regions, but the plots for Q = Te, X ≠ F are shaped differently. These latter plots also seem to be divided into two clear sets, however, the region where $b1$ and $b2$ are approximately equal is now at a large value of $b1$. Figure 2 shows a schematic view of the two sets of data points for both Q = Sb and Q = Te.

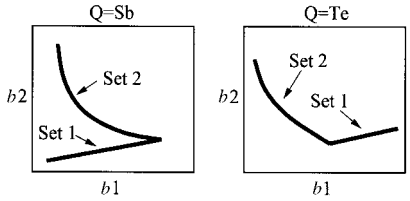

Figure 2. Schematic diagrams of the data sets for Q = Sb and Q = Te.

Fluorine is different, as usual. For Q = Sb there is a very sharply increasing region with only a few points when $b1$ has a value between 1.9 and 2.0 Å. This region may correspond to Set 2 . However, in general, it seems that intermolecular contacts between pnicogens or chalcogens and fluorine mostly occur at large values of $b2$; these contacts are more like van der Waals interactions than secondary bonds.[10]

In Figure 3 we plot the bond angle (θ) versus the bond-length asymmetry parameter, *asym* ($asym = (b2 - b1)/b1$). These plots share similarities: dense groupings of points with small *asym* and θ close to 180° (these are the members of Set 2). In general, as *asym* increases, the deviations from $\theta =$ 180° also increase. Another trend which can be seen in Figure 3 is a general narrowing of the distribution of points along the *asym* axis upon moving from Cl → Br → I.[11]

Scatter plots (not shown here) constructed for Q = As, Bi, and Se, although containing varying numbers of bond pairs, show similar features. The general trend of a narrowing of the distribution of bond asymmetries is also seen as Q moves down a column of the periodic table; that is the distribution for Q = Bi is narrower than that for Q = As.

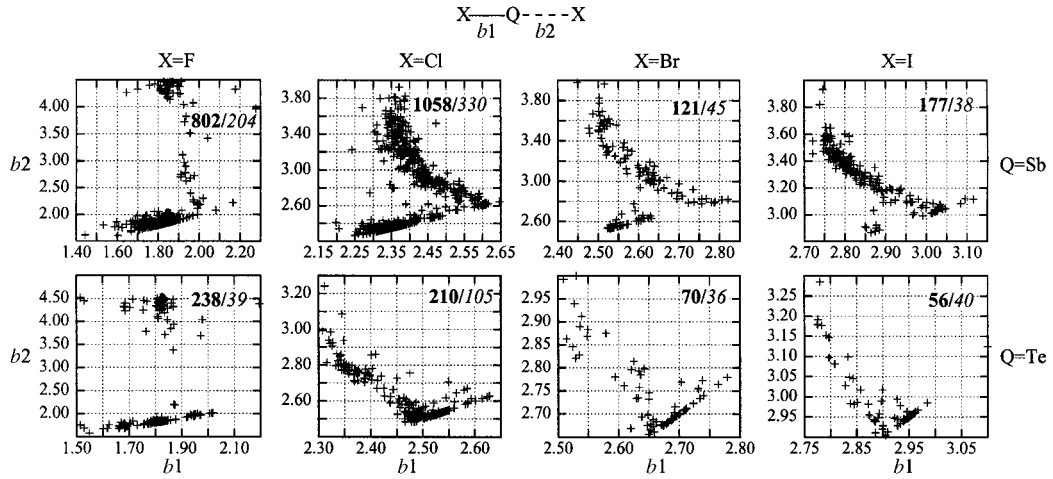

Figure 1. Scatter plots of the bond lengths $b2$ and $b1$ for the antimony– and tellurium–halide systems. The number in italics in each plot is the number of structures found in the database. The number in boldface is the number of distinct $b1$–$b2$ pairs.

The regularities in the large crystallographic data set are intriguing. To get a feeling for what is happening, we examine a selection of structures from the Q = Sb, X = Cl data set. We start at the short (low $b1$) end of Set 1. The $[SbCl_6]^-$ ion is well known—a CSD search turns up more than 200 distinct $[SbCl_6]^-$ units. For instance, the geometry of $[SbCl_6]^-$ when it is a counterion for the meth-

  1433-7851/98/3713-1888 $ 17.50+.50/0 *Angew. Chem. Int. Ed.* **1998**, *37*, No. 13/14

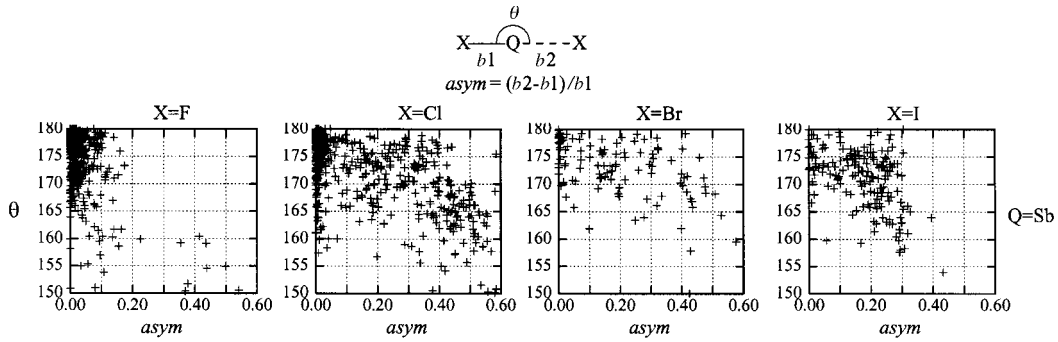

Figure 3. Scatter plots of the bond asymmetry parameter (*asym*) and angle θ for the antimony–halide systems.

yloxocarbonium ion is shown in **2**.[12] $[SbCl_6]^-$, isoelectronic to the familiar SF_6, is a hypervalent molecule with electron-rich three-center bonds.[13] The potential energy surfaces for distortions of these bonds are quite flat (more about this below), so we would expect the geometry of $[SbCl_6]^-$ to be sensitive to its environment in the crystal. Such effects can easily give rise to the 0.01 Å differences in bond lengths observed in **2**.[14, 15]

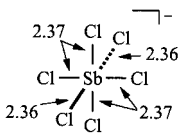

2

The Sb–Cl distances need not be so short, even if $b1 = b2$. An example is $SbPh_3Cl_2$.[16] This trigonal bipyramid structure has Sb–Cl distances of 2.46 and 2.47 Å. The surface for symmetrical hypervalent bonding must therefore be soft.

From the "long side" of the linear region of the Sb–Cl graph, past the point where Sets 1 and 2 merge, comes the $[SbCl_6]^{3-}$ ion found in tetrakis(dimethylammonium)hexachloroantimony chloride (**3**).[17] This interesting species is roughly isoelectronic to XeF_6 and exhibits both very long (2.65 Å) symmetrical Sb–Cl contacts and an asymmetrical (*asym* = 0.10) secondary bond. The antimony center here is in the +3 oxidation state and has a lone pair of electrons that should occupy the sixth site of an octahedron. The geometry of the secondary bond here violates one of Alcock's rules: the secondary bond should not lie in the same direction as a lone pair on the central atom.[1]

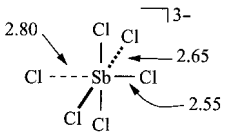

3

The bonding in these molecules can be described as being not very different from the many, and well-understood, triiodides.[4] The symmetrical I_3^-, $[SbCl_6]^-$, and $[SbCl_6]^{3-}$ ions are classic cases of electron-rich three-center bonding.[13] In the same way, the unsymmetrical cases can also be viewed as perturbed three-center systems. Alternatively, they may be seen as donor–acceptor complexes: the donor is a halide lone pair of electrons, the acceptor the only remaining σ* orbital of the I_2 molecule, or the Sb–Cl bond. Alcock's rules are often not followed.

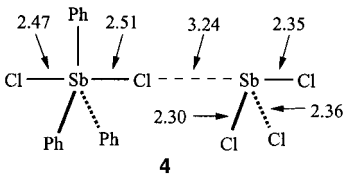

4

Another species that has Sb–Cl interactions falling into both Sets 1 and 2 is $SbPh_3Cl_2 \cdot SbCl_3$ (**4**).[18] The Cl-Sb-Cl system within the $SbPh_3Cl_2$ molecule here is quite similar to that in $[SbPh_3Cl_2]$ itself. The secondary contact (indicated with a thin dashed line) is both long and very asymmetric (*asym* = 0.38), but still shorter than an Sb–Cl van der Waals contact ($\approx$4.0 Å).[19] The geometry of the secondary contact is somewhat unusual, because it is not immediately clear from the geometry which molecule is acting as a donor and which is the acceptor. Both molecules have donor capabilities ($SbPh_3Cl_2$ through the lone pairs on the Cl atoms and $SbCl_3$ through the lone pair on the Sb^{3+} ion) and both have σ* levels which can act as acceptors. The secondary bond is parallel to the σ* orbitals of both the $SbPh_3Cl_2$ and $SbCl_3$ molecules. It seems there is no clear division in this intermolecular complex between the donor and the acceptor species. The Sb–Cl bond of 2.36 Å in the $SbCl_3$ molecule is also opposite a $SbPh_3Cl_2$ molecule (not shown in **4**). The shorter Sb–Cl contact (2.30 Å) on $SbCl_3$ is not involved in intermolecular interactions.

In the Te–Cl data set the bond pairs which are found in Set 1 are also clearly hypervalent: many of the bond pairs are from $[TeCl_6]^{2-}$ ions (isoelectronic to both XeF_6 and the $[SbCl_6]^{3-}$ species discussed above). The members of Set 2 are, once again, primarily intermolecular contacts.

Just from this small sampling of structures, the two sets found in the plots of Figure 1 can be interpreted. The systems which lie in Set 1 (with low asymmetry parameters and angles close to 180°) are best described as intramolecular electron-rich three-center bonds. Set 2 consists mainly of intermolecular and long intramolecular contacts: these are secondary bonds, best thought of as donor–acceptor interactions.[20] These conclusions can be extended to the other members of the pnicogen-halide and chalcogen–halide series.

The potential energy surfaces for distortions of a $[SbCl_6]^-$ octahedron were systematically explored by using density functional calculations. Three distortions, corresponding to the symmetric stretch in an octahedron, a symmetrical stretch of the axial bonds alone, and an asymmetric stretch of just one bond, were studied. The energy curves computed, *per bond distorted*, are nearly identical. In every case, the energy required to stretch an individual Sb–Cl bond by 0.15 Å is on the order of only 2 kcal mol^{-1}. Similar results are obtained for the isoelectronic species $TeCl_6$ and $[ICl_6]^+$. The surface for the distortion of $[ICl_6]^-$, isoelectronic to $[SbCl_6]^{3-}$ and $XeCl_6$, is even softer: a distortion of the I–Cl bond by 0.15 Å costs less than 1 kcal mol^{-1}. The surfaces for distorting these electron-rich three-center bonds are really flat.

  1433-7851/98/3713-1889 $ 17.50+.50/0

There are still some questions left unanswered about the plots of Figures 1 and 2. For example, why is it that the incidence of secondary bonding seems to decrease as Q or X move upwards in the periodic table[1] (Figure 1)? Why does the width of the distribution of the asymmetry parameter (*asym*) decrease as X changes from Cl → Br → I or as Q moves down a column of the periodic table? These two questions are intimately related and can be answered simultaneously, we believe.

If we focus on the members of Set 2 in Figure 1 (recall that these are the secondary contacts), there is a clear inverse correlation between secondary (*b*2) and primary (*b*1) bond lengths: as *b*2 becomes shorter, *b*1 gets longer. So, forming the secondary bond weakens the primary bond; an effect that an inorganic chemist would call a "*trans* influence". This is what we would predict based upon our donor–acceptor view of these interactions; increased secondary bond strength indicates increased donation into the antibonding orbitals (and thus weakening) of the primary bond.

Towards the top of the periodic table bonds tend be stronger—this effect is well known for primary bonds and presumably holds for secondary bonds as well. The delicate balance between two effects—bond strengthening and the competition between primary and secondary bonds—may change as we move up the periodic table, affecting in turn the nature of the secondary bonds observed. For example, as we pointed out above, the distribution of the bond asymmetry parameter for secondary systems changes with position in the periodic table. As either Q or X is moved up in the table, the width of the distribution of *asym* gets broader; a consequence of the secondary bonds getting longer relative to the primary bonds. Since bonds *b*1 and *b*2 are both of the same type (between the same types of atoms), the secondary bonds must be getting weaker relative to the primary bonds. Note that these comments are about general trends; it is possible to delve into the data sets and find specific counterexamples.

Finally, we would like to point out that there is no clear dividing line between secondary and hypervalent bonding in the systems that we have examined. For example, the curve of Set 2 in the Sb–Cl system (Figure 1) runs smoothly, without breaks, between $b2 = b1 = 2.65$ Å (this hypervalent contact is shown in **3**) and the higher regions where *b*2 is approximately 4.0 Å. There just is no logical place to divide the data that connect these two extremes.

Received: January 5, 1998 [Z 11326 IE]
German version: *Angew. Chem.* **1998**, *110*, 1989–1992

Keywords: donor–acceptor systems · halogens · hypervalent compounds · intermolecular interactions · secondary bonding

[1] N. W. Alcock, *Adv. Inorg. Radiochem.* **1972**, *15*, 1. In this work, Alcock proposed a set of rules governing the geometries of secondary bonds: 1. The geometry of the primary bonds of a molecule are determined using the Valence Shell Electron-Pair Repulsion (VSEPR) model. 2. Secondary bonds can form in line with primary bonds, in any direction not proscribed by the third rule. 3. Secondary bonds do not form in the same direction as a lone pair on the central atom.

[2] a) G. C. Pimentel, *J. Chem. Phys.* **1951**, *19*, 446. b) R. E. Rundle, *J. Am. Chem. Soc.* **1963**, *85*, 112. c) R. E. Rundle, *J. Am. Chem. Soc.* **1979**, *101*, 5057.
[3] a) H. A. Bent, *Chem. Rev.* **1968**, *68*, 587. b) C. K. Prout, J. D. Wright, *Angew. Chem.* **1968**, *80*, 688; *Angew. Chem. Int. Ed. Engl.* **1968**, *7*, 659.
[4] G. A. Landrum, N. Goldberg, R. Hoffmann, *J. Chem. Soc. Dalton Trans.* **1997**, 3605.
[5] N. Goldberg, G. A. Landrum, R. Hoffmann, unpublished results.
[6] G. A. Landrum, N. Goldberg, R. Minyaev, R. Hoffmann, *New J. Chem.*, in press.
[7] Similar directionality, interpreted also as weak donor–acceptor bonding, is important in determining the structure of gas phase aggregates. See, for example S. E. Novick, K. C. Janda, W. Klemperer, *J. Chem. Phys.* **1976**, *65*, 5115.
[8] R. H. Allen, O. Kennard, *Chem. Design Autom. News* **1993**, *8*, 31.
[9] The CSD contains an immense amount of information which has creatively been used in numerous studies to understand structural correlations, chemical reactivity, intermolecular interactions, and a variety of other properties falling under the general umbrella of "structural systematics"[14]. a) *Structure Correlation*, *Vols. 1, 2* (Eds.: H. B. Bürgi, J. D. Dunitz), VCH, Weinheim, **1994**. b) H. B. Bürgi, J. D. Dunitz, *Acc. Chem. Res.* **1983**, 153. c) S. L. Price, A. J. Stone, J. Lucas, R. S. Rowland, A. E. Thornley, *J. Am. Chem. Soc.* **1994**, *116*, 4910. d) J. P. Lommerse, A. J. Stone, R. Taylor, F. H. Allen, *J. Am. Chem. Soc.* **1996**, *118*, 3108. e) W. Clegg, R. J. Errington, G. A. Fisher, D. C. R. Hockless, N. C. Norman, A. G. Orpen, S. E. Stratford, *J. Chem. Soc. Dalton Trans.* **1992**, 1967.
[10] For another recent study of structural correlations in hypervalent systems containing fluorine, see V. A. Blatov, V. N. Serezhkin, Yu. A. Buslaev, Yu. V. Kokunov, *Zh. Neorg. Khim.* **1997**, *42*, 1941.
[11] This narrowing is not solely caused by the fact that bond lengths tend to increase upon moving down in the periodic table. The search criteria used (with a maximum *b*2 length of 4.5 Å) allow for asymmetry parameters as large as 0.6 when $b1 = 2.8$ Å. These large asymmetries are just not observed in the Sb–I data set, and are uncommon in that for Sb–Br.
[12] J. M. Le Carpentier, R. Weiss, *Acta Cryst. B* **1972**, *28*, 1421.
[13] The bonding in $[SbCl_6]^{q-}$ (q = 1,3) merits a more detailed discussion (for an introduction see T. A. Albright, J. K. Burdett, M. H. Whangbo, *Orbital Interactions in Chemistry*, Wiley, New York, **1985**, Ch. 14). The influence of electron count and the nature of the atoms involved on the propensity for symmetric and asymmetric distortions in hypervalent systems is being studied by H.-B. Bürgi and the authors.
[14] a) A. G. Orpen, *Chem. Soc. Rev.* **1993**, 191. b) A. Martín, A. G. Orpen, *J. Am. Chem. Soc.* **1996**, *118*, 1464.
[15] Recognizing this fact, we will only present bond lengths with three significant figures, despite the occasionally much smaller (and perhaps overly optimistic) standard deviations reported by crystallographers.
[16] M. J. Begley, D. B. Sowerby, *Acta Cryst. C* **1993**, *49*, 1044.
[17] F. Knodler, U. Ensinger, W. Schwarz, A. Schmidt, *Z. Anorg. Allg. Chem.* **1988**, *557*, 208.
[18] M. Hall, D. B. Sowerby, *J. Chem. Soc. Dalton Trans.* **1983**, 1093.
[19] A. Bondi, *J. Phys. Chem.* **1964**, *68*, 441.
[20] As we have shown elsewhere,[4] while electron-rich three-center and donor–acceptor bonding have been treated as distinct approaches to understanding electronic structure, they are easily brought into correspondence. The equivalence of these two approaches may be useful in rationalizing old and devising new chemistry.

  1433-7851/98/3713-1890 $ 17.50+.50/0